J Fluoresc (2011) 21:275–288
DOI 10.1007/s10895-010-0715-0

ORIGINAL PAPER

Tryptophan-Tryptophan Energy Transfer and Classification of Tryptophan Residues in Proteins Using a Therapeutic Monoclonal Antibody as a Model

Veysel Kayser · Naresh Chennamsetty · Vladimir Voynov · Bernhard Helk · Bernhardt L. Trout

Received: 14 August 2010 / Accepted: 8 September 2010 / Published online: 1 October 2010

Abstract Intrinsic tryptophan (Trp) fluorescence is often used to determine conformational changes of proteins. The fluorescence of multi-Trp proteins is generally assumed to be additive. This assumption usually holds well if Trp residues are situated at long distances from each other in the absence of any excited state reactions involving these residues and therefore when energy transfer does not occur. Here, we experimentally demonstrate energy transfer among Trp residues and support it by a Master Equation kinetic model applied to a therapeutic monoclonal antibody (mAb). The mAbs are one of the most studied and important biologics for the pharmaceutical industry, and they contain many Trp residues in close proximity. Understanding mAb fluorescence is critical for interpreting fluorescence data and protein-structure relationships. We propose that Trp residues could be categorized into three types of emitters in the mAbs. Experimentally, we categorize them according to solvent accessibility based on dependence of their fluorescence lifetime on the external quencher concentration and their emission wavelength. Theoretically, we categorize with molecular dynamics simulations according to their solvent accessibility. This method of combinatorial mapping of fluorescence characteristics can be utilized to illuminate structural aspects as well as make comparisons of drug formulations for these pharmaceutical proteins.

Keywords Energy transfer · Energy migration · Förster energy transfer · FRET · Monoclonal antibody · Tryptophan · Tryptophan fluorescence · Master equation · Kinetic model · Tryptophan classes · MD simulations · SAA

Electronic supplementary material The online version of this article (doi:10.1007/s10895-010-0715-0) contains supplementary material, which is available to authorized users.

V. Kayser · N. Chennamsetty · V. Voynov · B. L. Trout (✉)
Department of Chemical Engineering,
Massachusetts Institute of Technology,
Cambridge 02139 MA, USA
e-mail: trout@mit.edu

B. Helk
Novartis Pharma AG,
CH-4057 Basel, Switzerland

Background

The intrinsic fluorescence of proteins has been widely utilized to assess protein structure, stability and dynamics. Lately, fluorescence resonance energy transfer (FRET) has attracted much attention because it provides detailed information about the conformation of bimolecules [1–5]. Two types of FRET have been identified in the literature: FRET among different molecules (hetero-FRET) and FRET among identical molecules (homo-FRET). Although hetero-FRET has extensively been studied, homo-FRET has attracted less interest. For instance, energy transfer among Tryptophan (Trp) residues is studied only for a few proteins [1, 4–13] and is actually not frequently observed because of the relatively low quantum yield of Trp, the random spatial distribution of Trp residues in the protein structure and the very short Förster distances, typically ~5–16 Å [1, 5, 14–19].

Proper interpretation of complex fluorescence of Trp in proteins is of great importance in order to exploit FRET as a probe in protein folding and aggregation studies wherein achieving resolution at the individual Trp amino acid level is highly desirable. For instance, it would be very helpful to know whether any excited state reaction induces changes to the intrinsic fluorescence of these proteins.

The photophysics of the Trp residue in single Trp proteins [5, 20–24] is known quite well compared to that of multi-Trp proteins [25]. However, the majority of biotechnologically relevant proteins, [26–29] especially monoclonal antibodies (mAbs), have more than one Trp residue, resulting in complex fluorescence behavior due in part to energy transfer effects and in part to the unusually high dependence of Trp fluorescence to the polarity and viscosity of its environment [5, 20–24]. The fluorescence emission spectrum of Trp residue is broad with a central wavelength of ~350 nm [20, 21, 30] if it has a polar environment or is free to undergo relaxation motion without much restriction, similar to the Trp amino acid in aqueous phase, in melittin [20] or in glucacon [31]. By contrast, the Trp fluorescence spectrum is blue-shifted, quite narrow and very structured if it has a very hydrophobic or restricted environment, similar to that of Trp in vitrified nonpolar solvents [5, 23, 32, 33]. In fact, this blue-shifted emission is almost the mirror image of the ^1L_b absorbance dipole. In general, ^1L_a is the main emitting dipole, but both dipoles ^1L_a and ^1L_b contribute to the absorbance [34]. ^1L_a roughly lies from the center of the indole part of Trp to the nitrogen atom and ^1L_b is approximately perpendicular to this dipole. The ^1L_a dipole exhibits a red-shifted emission and primarily changes its size and direction upon excitation, and, thus, it is very sensitive to its vicinity and strongly influenced by polar environments and surrounding molecules that may act as quenchers. On the other hand, the ^1L_b dipole is affected by its surrounding polarity to a lesser extent thereby exhibiting a blue-shifted fluorescence. In addition to external quenchers such as acrylamide, as is shown here, neighboring molecules can also quench Trp fluorescence effectively, as well as contributing to the polarity of Trp. Phenylalanine (Phe) residues, methyl groups, peptide bonds themselves, electrophiles, e.g. amino groups, and even carboxyl groups, are all potential quenchers [5, 35–41].

Antibodies usually have many Trp residues, which are randomly distributed. Some are on the protein surface, and, thus, are very polar and solvent accessible; and others are located in the interior of the protein with very little or no interaction with solvent molecules. These Trp residues have very different fluorescence emission because of their different surroundings. This property in principle can be exploited to gather information about the dynamics of local regions of the mAb domains, if the Trp fluorescence could be decomposed into individual residues, or at least if they could be classified into distinctive classes [42–46]. Burstein and co-workers have proposed Trp classes based on their emission behavior and their environment [42, 44, 45]. Recently, they demonstrated that five of the Trp residues in a myosin subfragment are involved in ATP-induced fluorescence change [43]. It is possible that this classification and information about the orientational freedom of Trps could be used to assess the protein structure, stability and dynamics [43]. In addition, Trp fluorescence is currently assumed to be additive in the multi-Trp proteins, though this outlook might be altered once the individual Trp residue dynamics are elucidated better in the future.

We have used time-resolved and steady-state fluorescence spectroscopy to study the Trp excited-state dynamics in a therapeutic human IgG1 antibody (Fig. 1(a)). Acrylamide quenching was used to examine the Trp solvent accessibility of different Trp classes. We found that only the slowest emission decay was quenched, while the fast decay hardly changed with the acrylamide concentrations we used. Trp fluorescence lifetimes col-

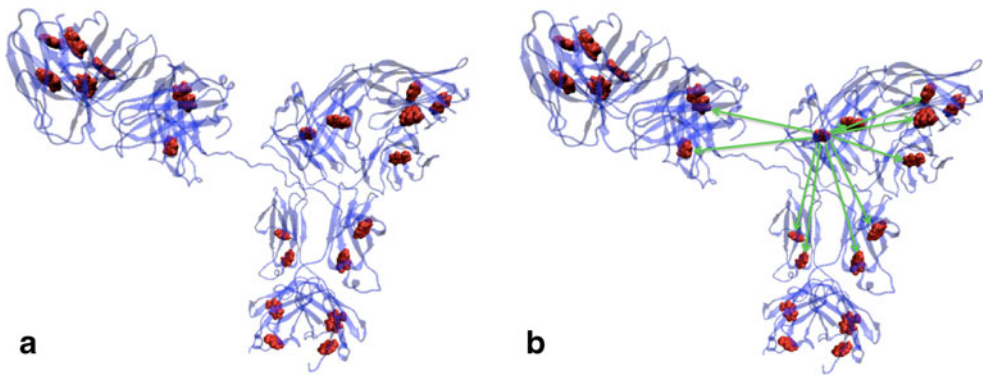

Fig. 1 **a** mAb structure (*blue ribbons*) and Trp positions (*red spacefilled structures*) from X-ray crystallographic data. The structure of the Fab fragment was obtained from Novartis Pharma, and the Fc fragment structure is from another human IgG1 [51] (pdb 1HZH). The full mAb structure was constructed by aligning these fragments using 1HZH as a template. **b** Schematic of the energy transfer simulation where the excited state energy of one Trp can be transferred to any other Trp residue. The largest 10 transfer pathways from one of the Trps are shown

lected at different emission wavelengths also indicated three types of Trp environments: One type fluoresces with maximum intensity at 350 nm, other type fluoresces around 320 nm and the last one has fluorescence maximum intensity of around 330–340 nm.

We also used fluorescence depolarization to probe energy transfer among Trps. Fluorescence emission is polarized if the excitation light is polarized, unless the fluorophore undergoes a rapid rotational motion or the excited state energy is transferred from one fluorophore to another or both. The rotational freedom of Trp residues can be minimized by increasing the solution's viscosity. In this case, the presence of depolarization suggests the presence of energy transfer among Trp residues [5, 47–50]. Our depolarization results via anisotropy measurements show that there could be energy transfer from buried Trps (at high energy) to the surface exposed Trps. Therefore, energy transfer among the Trp residues are considered and investigated by a Master equation kinetic model which incorporates the interactions, a specific set of which are shown in Fig. 1(b). We further calculated solvent-accessibility with all atom molecular dynamics (MD) simulations for each Trp residue. Moreover, we studied the evolution of Trp-Trp distances with MD simulations. Results from simulations are used in the interpretation of the Trp environments in the experimental observations.

Materials & Methods

Chemicals and Protein

KH_2PO_4, K_2HPO_4, H_3PO_4 and NATA were purchased from Sigma-Aldrich. All chemicals were the highest possible grade available and were used as received without further purification. The mAb was a therapeutic human IgG1 and supplied by Novartis with 150-mg/ml concentration in 20 mM His buffer.

Fluorescence

Steady-State Measurements A Fluorolog3 from Jobin-Horiba-Yvon (NJ, USA) was used for fluorescence emission measurements. Tryptophan was excited at 295 nm, and its emission was recorded at 305–450 nm with 1-2 nm slits. All spectra were corrected for background, dark count and instruments response. The mAb concentration was 0.5 mg/ml unless otherwise stated.

Time-Resolved Measurements An Edinburgh Instruments (Edinburgh, UK) LifeSpec-ps spectrometer was used for Trp lifetime measurements. Fluorescence lifetimes and anisotropy were measured by time-correlated single photon counting (TCSPC) [52]. The excitation source was a picosecond (ps) light-emitting diode (LED) emitting at 295±10 nm with 2 MHz repetition rate. The detector was a Hamamatsu H5773, and instrument response was ~200 ps at FWHM. A high-pass cut-off filter (Newport FSQ-WG320) was used to block excitation light. A monochromator was used to select the desired fluorescence wavelength between 320 and 360 nm, depending on the experiment. Iterative reconvolution fits to the fluorescence lifetime data were performed with IgorPro or FAST software. A Marquardt-Levenberg algorithm is used in IgorPro, while FAST employs a non-negative truncated singular value decomposition algorithm for least-squares fits. Goodness of the fit was judged by reduced chi-squared and residuals. Fluorescence lifetimes were calculated as sum of exponentials using the following equation

$$I(t) = \sum_{i=1}^{4} \alpha_i \exp(-\tau_i/t) \tag{1}$$

where τ is the fluorescence lifetime and the α_i are the pre-exponential factor related to the fraction of each lifetime. The average lifetime is given explicitly by

$$\langle \tau \rangle = \frac{\sum_{i=1}^{4} \alpha_i \tau_i^2}{\sum_{i=1}^{4} \alpha_i \tau_i}. \tag{2}$$

The fluorescence anisotropy was calculated as

$$r(t) = \sum_{i=1}^{2} \beta_i \exp\left(-\theta_i/t\right), \tag{3}$$

where θ_i are the rotational correlation times, and the β_i are constants.

Decay Associated Emission Spectra (DAS) DAS was calculated by measuring the fluorescence lifetime (as described above) at different emission wavelengths between 320 nm and 360 nm. The pre-exponential terms of these lifetimes were correlated with emission spectrum to calculate the fractional intensity ($I_i(\lambda)$) of the i^{th} component according to $I_i(\lambda)=I_{Total}\, f_i(\lambda)$, where $f_i(\lambda)$ is the fraction and I_{Total} is the total fluorescence. Measured fluorescence decays at different wavelengths were analyzed with global analysis by linked fluorescence lifetimes.

Fluorescence Quenching with Acrylamide mAb was diluted down to 0.5 mg/ml, acrylamide was added, and the solution was kept overnight for equilibration. Fluorescence emission

and lifetime were recorded as mentioned above. Data was analyzed according to the following Stern-Volmer (SV) equation

$$\frac{\tau_0}{\tau} = \frac{F_0}{F} = 1 + k_q \tau_0 [Q], \tag{4}$$

where F_0 and F are the fluorescence emission in the absence and presence of acrylamide respectively. τ_0 and τ are the fluorescence lifetimes of the same solutions. k_q is the bimolecular quenching constant, and Q is the quencher concentration. Emission peak areas were used for calculating the ratio in this equation. In addition, we shall assume that $\tau_0 = <\tau>$ for multi-Trp proteins.

The SV equation is strictly true for dynamic quenching of single Trp proteins in the absence of any static quenching. For multi-Trp proteins, however, it is possible that $\tau_0/\tau \neq F_0/F$, and therefore the quenching results from steady-state and time-resolved measurements may not agree with each other. This is because, while steady-state measurements can show both dynamic as well as static quenching, time-resolved measurements are only affected by the dynamic quenching, since Trp residues that have a contact distance with a quencher would not be fluorescent and thus not be detected in the experiment. This phenomenon is observed only as the reduction in the fluorescence spectrum [15].

Trps could have different quenching constants for each emitter group in multi-Trp proteins. In such cases, F_0/F versus the Q concentration could be nonlinear, and a modified Stern-Volmer plot would be more appropriate to analyze the data [53]. Assuming that there is more than one emitter population, solvent accessible/inaccessible fraction of the emitters could be found by following equation.

$$F_0/(F_0 - F) = 1/f_i + 1/\left(f_i K_Q [Q]\right) \tag{4.1}$$

This equation can be used for determining the fractional quenched fluorescence (f_i). K_Q is the intercept/slope ratio, and other parameters are as described above.

Equilibrium and kinetic GuHCl Unfolding The fluorescence signals of denatured mAb were recorded with the Fluorolog3 fluorescence systems described above. The excitation wavelength was 295 nm, and Trp emission was collected between 300 and 450 nm with 1 nm increment and 1 nm slits. The background was subtracted from all measurements, and other corrections such as instrument response and dark count etc. were performed as necessary. For equilibrium unfolding experiments, 1-mg/ml mAb was incubated with GuHCl for at least 24 h, and the same concentrations were used for the kinetic measurements. Kinetic data was analyzed with (multi)-exponential fit, and the goodness of the fit was judged by residuals and chi-square. The unfolded fraction was calculated as a function of GuHCl concentration according to $f_u = (I–I_N)/(I_U–I_N)$, where I_N, I_U are the measured native and unfolded intensities, respectively. The protein was assumed to be totally folded and unfolded in the absence and presence of the highest denaturant concentration, respectively.

Förster Resonance Energy Transfer The rate constants of the energy transfer among Trp residues were calculated via [54–56]:

$$k_{EnT} = \frac{\ln(10) 9000 \phi_D \kappa^2}{128 \pi^5 N n^4 \tau_D r^6} \int F_D(\lambda) \varepsilon_A(\lambda) \lambda^4 d\lambda = \frac{\phi_D \kappa^2}{\tau_D} \left(\frac{r_0}{r}\right)^6, \tag{5}$$

where ϕ_D is the quantum yield of unquenched Trp, κ^2 is the relative donor-acceptor orientation, N is Avogadro's number, n is the refractive index of the environment, τ_D is the unquenched fluorescence lifetime of Trp, r is the donor-acceptor distance, F_D is the area normalized donor fluorescence, ε_A is the extinction coefficient of Trp, λ is the wavelength, and r_0 is the Förster distance, that at which half of excited molecules undergo energy transfer. The overlap integral was calculated from the normalized emission of the donor and absorbance of acceptor. The overlap integral can be calculated from steady-state spectra because energy transfer usually is longer than the excited state relaxation times.

Energy Transfer Simulations by Master Equations Supposing that the energy transfer occurs many times in consecutive steps in a weak dipole-dipole (Förster) coupling limit, the time evolution of the system can be simulated with help of the kinetic master equation approach, if the protein structure is known. Also, the fluorescence of the donor would be depolarized should there be energy transfer as mentioned earlier. Assuming that every Trp, i, can transfer its excitation energy to all others, j, the rate coefficient of the transition from i to j, k_{ij}, for the energy transfer can be calculated from the overlap integral, obtained from experimental data and the distances and relative orientations between the molecules. For simplicity, we shall further assume that each Trp fluoresces with the same emission decay, τ, and that the transitions should occur independently within any given time. With these assumptions, the population (P) of the molecule i for any

given time can be calculated via the following coupled kinetic equations.

$$MP_i = \frac{dP_i}{dt} = \sum_{j\neq i}^{N} P_j k_{ji} - \sum_{i\neq j}^{N} P_i k_{ij} - k_f P_i$$

where $k_f = 1/\tau$ is the reciprocal emission decay and N is the number of Trp's in the protein. The first term in this equation treats the transfer from any Trp i to Trp j; the second term is the loss of population caused by the transfer of energy from Trp i to any other Trp j. The last term is loss because of fluorescence. We can solve these rate equations simultaneously for all Trps by the eigenvalue-eigenvector method. For this we need to construct a square matrix, of size N x N, whose elements are denoted by:

$$M_{ij} = \begin{cases} k_{ij} & i \neq j \\ -\sum_{i\neq j} k_{ij} & i = j \end{cases}$$

or

$$M_{ij} = -(1-\delta_{ij})k_{ij} - \delta_{ij}\left[\sum k_{ij}(1-\delta_{ij}) + k_f\right],$$

where δ is the Kronecker delta. According to the description above, the matrix has positive off-diagonal terms that represent the transfer from Trp i to Trp j, and negative diagonal terms that denote the population decrease of Trp i. For a given column, the sum of the off-diagonal terms has the same magnitude as that of the diagonal terms. This notion ensures that population changes are due to transfer as well as fluorescence only if $i \neq j$, and the population loss occurs only by fluorescence if $i = j$. For simplicity, we shall assume that only fluorescence and/or energy transfer depopulates the excited state. An analytical solution of this matrix can be achieved by diagonalizing it and obtaining eigenvalues and corresponding eigenvectors. We can rewrite the time-evolution of the population of Trp i as

$$P_i(t) = D^{-1}\exp(\lambda_i t)DP_0$$

where λ represents the eigenvalues, D are the eigenvectors, D^{-1} is its inverse, and P_0 is the initial population column vector. Each Trp was excited in turn and the populations were summed to get the evolution of the total average population with time. These populations were in turn used to calculate the fluorescence anisotropy as $r(t) = (I_V(t) - I_H(t))/I_T$, where I_V and I_H are vertically and horizontally polarized emission intensities respectively, and I_T is the total emission intensity given by $I_T = I_V(t) + 2I_H(t)$. Emission from ^1L_b is not justified in this case; therefore, Trp emission was assumed to be from the dipole ^1L_a, which lies almost parallel to the absorption dipole.

Molecular Dynamics Simulations Molecular dynamics simulations were performed for the full mAb using an all atom model with explicit solvent. The starting structure for the simulation were obtained from the X-ray structures of individual Fab and Fc fragments; The Fab fragment structure was obtained from Novartis Pharma AG, and the Fc structure from that of another IgG1 antibody, 1HZH [51]. The structure of a full antibody was then obtained by aligning the Fab and Fc fragments using 1HZH structure as a model template. This structure was then used to perform explicit atom simulations for 30 ns. The Cys residues in the resulting mAb were all involved in disulphide bonds, including the ones in the hinge region. We have used a G0 glycosylation pattern for our simulations, since this is the most common glycosylation pattern observed in antibodies.

We used the CHARMM simulation package [57] for set-up and analysis and the NAMD package [58] for performing the simulations. The CHARMM fully atomistic force field [59] was used for the protein and TIP3P [60] solvent model for water. The simulations were performed at 298 K and 1 atm in the NPT ensemble. The parameters for the sugar groups involved in glycosylation of the Fc fragment were derived to be consistent with the CHARMM force field, from the CSFF force field [61]. The protonation states of Histidine residues at pH-7 were decided based on the spatial proximity of electro-negative groups. The full antibody was solvated in an orthorhombic box with periodic boundary conditions in all 3 directions, and a water solvation shell of 8 Å was used. The resulting total system size was 202130 atoms. Sufficient ions were added to neutralize the total charge of the system as required by the Ewald summation technique used to calculate the electrostatic contribution.

After the antibody was solvated, the energy was initially minimized with Steepest Descent (SD) by fixing the protein and allowing the water to relax around it. Then, the restraints were removed, and the structure was further minimized with SD and Adopted Basis Newton–Raphson (ABNR). The system was then slowly heated to room temperature with 5^0C increments every 0.5 ps, using a 1 fs time step. The system was then equilibrated for 1 ns before starting the computation of the various properties from the simulation. The configurations were saved every 0.1 ps during the simulation for further statistical analysis.

Results & Discussion

Trp Fluorescence as a Function of Acrylamide Concentration and Emission Wavelength Acrylamide is a water-soluble surface quencher, which does not penetrate into the protein matrix [15, 62, 63]. Thus, we assume that only the surface-exposed Trps are quenched by acrylamide. The

results of acrylamide quenching experiments for both time-resolved and steady-state fluorescence are shown in Fig. 2 (a) and (b), respectively. In Fig. 2(a), the fluorescence lifetime is plotted for various acrylamide concentrations and is fitted by a sum of three exponentials. The complex decay is probably due to the existence of many Trp residues with different environments in the protein. Detailed examination of the fluorescence lifetime reveals that the longest decay component quenches more than others even at the lowest acrylamide concentration (Fig. 2(a) and Supplementary Table 1). We attribute this lifetime to Trp residues on the surface, one of the three proposed Trp classes. These surface Trps are not constrained in their motion, are highly solvent exposed, and, thus, easily come into contact with acrylamide.

Fluorescence lifetime also depends on probed emission wavelength (Supplementary Table 1). Emission decay measured at 320 nm has one fast component of ~250 ps and two slower decay components. The fast decay is the least affected by the presence of quencher (Fig. 2(a) and Supplementary Table 1). Contribution of this fast lifetime to the total fluorescence is about 9% in the absence of quencher and about 13% in the presence of the quencher at 320 nm emission (Supplementary Table 1). This fast decay also does not contribute considerably to the emission at longer wavelengths. For example, the fast decay contributes only about 1% to the total emission when it is collected at 360 nm in the absence of acrylamide. Assuming that submolecular local changes are reflected on the fluorescence spectrum, accompanying emission of Trps with this fast decay should indicate no solvent exposed geometry to the bulk water. Therefore, their fluorescence decay as a function of emission wavelength is dominant only around 320 nm. These Trps should posses a very hydrophobic rigid environment in the interior of the protein matrix, and display characteristic blue-shifted fluorescence emission [5, 23, 32, 33, 62]. In proteins, it is not uncommon that buried Trps have the fastest decays, [5, 23, 32, 33, 62] though many exceptions exist. For example, human serum albumin (HSA) has one buried Trp residue with ~6–8 ns fluorescence lifetime [64]. The fast decay is probably due to interactions with neighboring side chains or with the peptide backbone via charge transfer. We classify these buried Trp residues as another Trp class.

We also observe heterogeneity of Trp environments from the quencher concentration dependence of the fluorescence emission spectrum (Fig. 2(b, c)). Surface Trps are quenched with acrylamide, and their fluorescence emission is reduced and eventually diminishes with increasing quencher concentration (Fig. 2(b)). Consequently, the protein fluorescence spectra shifts to the blue with increasing acrylamide concentration because now the less fluorescent buried Trps become the dominant emitting species (Fig. 2(c)). These results are reminiscent of Trp classes in self-assembling peptides [5] and smaller globular proteins [53, 65–68].

Figure 2(d) shows a Stern-Volmer plot and the bimolecular quenching constant, k_q. The Stern-Volmer plot is not linear but has some downward curvature at low [Q]. This type of downward curvature usually represents the coexistence of both dynamic and static quenching or indicates that some of the emitters are not accessible to the quencher molecules. In static quenching, the Trp fluorescence is quenched as soon as it is excited if there are nearby acrylamide molecules. The bimolecular quenching constant is $k_q = 2.70 \times 10^8\ M^{-1} s^{-1}$ (Fig. 2(d)) and fractional quenching is calculated to be 52% according to the modified Stern-Volmer equation [53] (Fig. 2(e)).

The last class of Trp residues consists of partially buried Trp inside the protein in a fairly constrained position. Acrylamide quenching results (Supplementary Table 1 and Fig. 2(f)) show that these partially buried Trps should have some solvent exposure and, thus, are not quenched as much as the surface Trps but quenched more than the totally buried Trps. Their emission spectrum should be blue shifted to around 330–340 nm as in other proteins with moderately buried Trps [45]. Emission decays of these partially buried Trps are also relatively shorter than the solvent exposed Trps (Supplementary Table 1), probably due to quenching with both acrylamide and surrounding residues. These partially buried Trps could be potential donors in energy transfer reactions, since they have higher excited state energies compared to those of the surface Trps. They also could act as acceptors if the buried Trps behave as donors.

Fluorescence Lifetime as a Function of Emission Wavelength and Decay Associated Spectra (DAS) Other evidence for the longest lifetime belonging to the surface Trps comes from the wavelength dependence of the fluorescence decay (Fig. 2(f)). The surface Trps are relatively mobile and are in a very polar environment, and, thus, their emission is around 350 nm. The fluorescence lifetime of these surface Trps quench the most in the presence of acrylamide. This can be observed when the fluorescence decay is specifically recorded at long wavelengths (~360 nm) (Fig. 2(f)). On the contrary, this longest emission decay contributes a smaller percentage to the total decay when the fluorescence lifetime is recorded at low wavelengths (~320 nm) (Fig. 2(f)).

Trp residues emit at relatively long wavelengths when they have polar environment because they can lower their energy by interacting with surrounding solvent molecules. In addition, their fluorescence lifetime is the longest in this type of environment [15]. Therefore, we have assigned the longest lifetime (3.6 ns) to the surface Trp residues, which have the most polar environment in the protein. On the other hand, Trp residues in the vicinity of nonpolar regions, such as the protein interior, have very short fluorescence

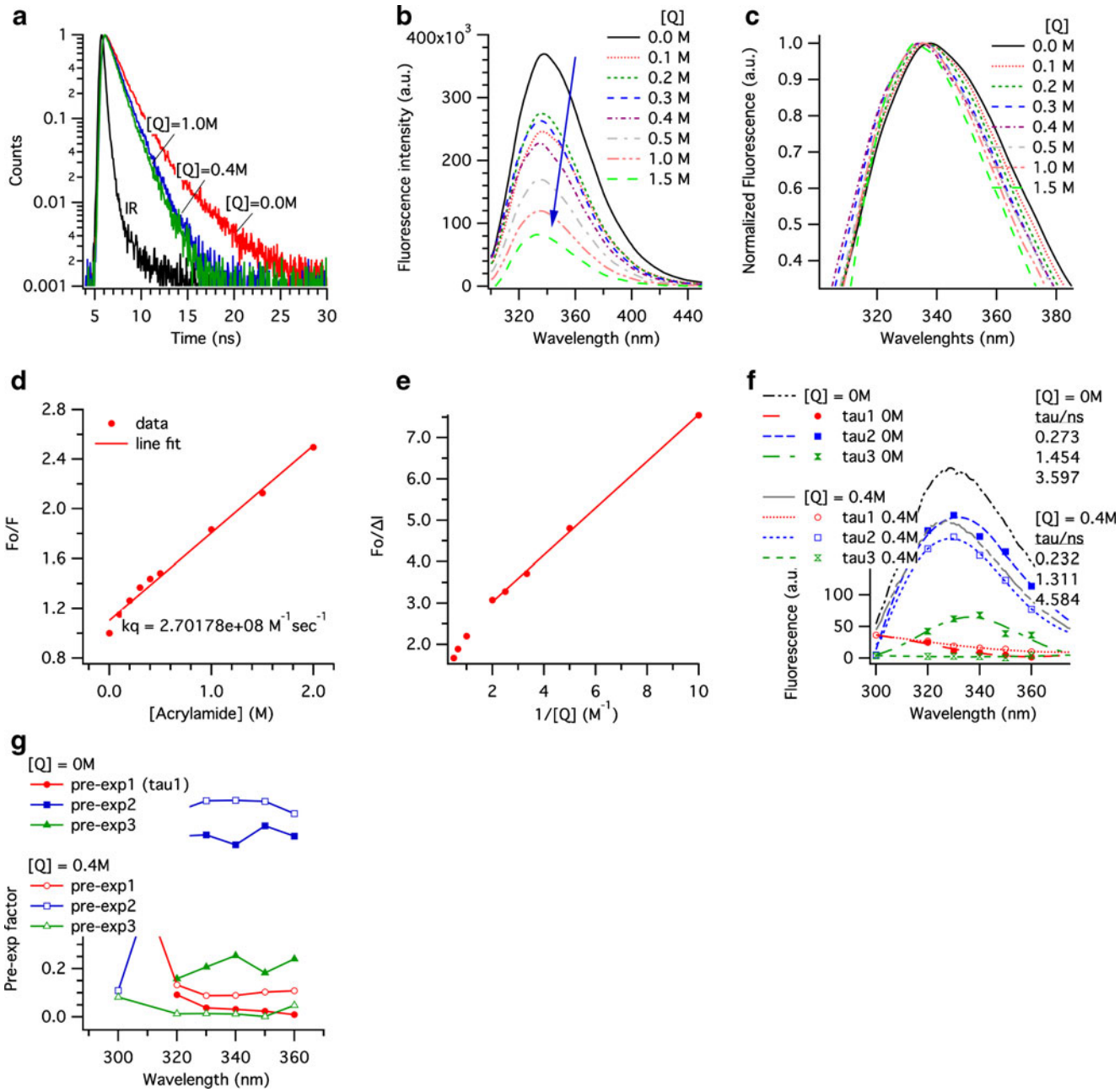

Fig. 2 **a**, **b** Quencher concentration dependence of fluorescence lifetime and emission spectra, respectively. Fluorescence decay analysis results are shown in Supplementary Table 1. **c** Normalized fluorescence spectra showing the emission shift with quencher concentration. Buried Trp residues emit at shorter wavelenghts and contribute more to mAb emission giving rise to a shifted emission that is dependent upon acrylamide (*Q*) concentration. **d** Stern-Volmer plot. The bimolecular quenching constant is shown. **e** Fractional quenching of emission (52%). Only the linear portion is shown. **f** DAS spectra with quencher concentration. Emission from shorter lifetime (0.27 ns) is not affected by quencher, while the emission from the longest lifetime (3.6 ns) is quenched heavily. Partially exposed Trps with ~1.4 ns lifetime are also quenched but not as much as Trps with 3.6 ns lifetime. This indicates that the longest emitters are located on the surface. In contrast, the shortest lifetime emitters (270 ps) are buried inside the mAb, a region without solvent accessability. *Inset:* fluorescence lifetimes that were used to calculated DAS in the presence and absence of the quencher. **g** Wavelength dependence of the pre-exponential factors from the three exponential fit. The pre-exponential factor of the surface Trps (*longest lifetime*) is lower in the prescence of the quencher, indicating that the contribution to the total fluorescence from these Trps is minimal when the quencher is present

lifetimes, and their fluorescence is usually blue shifted. Thus, we think the shortest fluorescence lifetime (0.27 ns) in our three exponential fit results are associated with the interior Trps, which are not prone to quenching by acrylamide. Indeed, this is what we observe from DAS as shown in Fig. 2(f). Emission from the longest lifetime (3.6 ns) is quenched almost totally whereas emission from the shortest lifetime (0.27 ns) does

not change in the presence of acrylamide (fractional contribution of 3.6 ns component is negligible, see Fig. 2 (g)). Partially solvent exposed Trp residues (1.45 ns component—squares) are also prone to acrylamide quenching at sufficient quencher concentrations (not shown), and their emission is influenced less than that of the surface residues (Fig. 2(f)).

Fluorescence Emission and Decay as a Function of GuHCl Concentration The Trp fluorescence change due to protein unfolding both as a function of GuHCl concentration and as a function of time at high GuHCl concentrations is shown in Fig. 3. The midpoint of unfolding occurs around 3 M GuHCl (Fig. 3(a–b)). A two-state model could not be fitted adequately to this data, indicating the existence of unfolding intermediates (Fig. 3(c)). The intermediate can be observed as a plateau at 4–5 M GuHCl in what would otherwise be a smooth sigmoid curve. Moreover, an indication of intermediates can also be seen in the kinetic unfolding measurements at early times (0–200 s) (Supplementary Figure 2). There is evidence from DSC results that (not shown) the CH2 region of Fc is unfolded first in the absence of large hydrophobic patches [69]. Thus, we could speculate that the intermediate by GuHCl unfolding might be due to unfolding of its CH2 region, though temperature and denaturant unfolding may also occur with a totally different mechanism.

Fluorescence decay as function of GuHCl concentration is shown in Fig. 3(d). The fluorescence lifetime data could be analyzed with only two exponentials in GuHCl solutions (at both 3 M and 6 M). Trp emission decays become less complex and become almost the same (Table 1). This is contrary to the case of the native protein where a three exponential curve fit is necessary for an acceptable fit. When the protein is unfolded, the majority of the Trp residues are exposed to the solvent molecules to a similar degree. Consequently, their fluorescence properties should be comparable due to having similar environments. Especially, the short decay disappears upon unfolding, indicating that this short lifetime belongs to the buried Trp residues. These results also demonstrate that buried Trp fluorescence should be quenched in the native protein by some sort of excited state reaction.

Discussion of MD Simulation Results The molecular dynamics simulations also identify three types of Trp residues, categorized by their solvent accessible area (SAA), see Figs. 4 and 5. For example, from Fig. 4(a) we could categorize that Trp residues that display solvent accessible area (SAA) levels of 10 Å^2 or above as "surface", those with SAAs of 5–10 Å^2 as "partially exposed", and those with SAAs≤5 Å^2 as "buried". Also, it would be very difficult to identify a given fluorescence signal for a given Trp; the simulation results indicate that each Trp in a given category of SAA should also exhibit corresponding experimental properties, see Table 2. The results of MD simulation are consistent with our acrylamide quenching results as discussed in page 12.

The MD results can also be analyzed to indicate whether or not energy transfer might occur. This is generally considered to be a possibility in situations where the Trp-Trp distance is less than 10–15 Å [1, 5, 14–19]. Distances between Trp residues from the crystal structure seem to be quite long, which would not allow Trp-Trp energy transfer to occur. However, protein dynamics from simulations show that Trp residues are quite mobile and the distances

Table 1 Tryptophan fluorescence decay analysis as a function of GuHCl concentration

[GuHCl] (M)	exp num	α	f	τ (ns)	<τ>(ns)	χ^2
0	1	0.08	0.66	1.23	1.81	1.39
	2	0.02	0.34	2.82		
	1	0.03	0.06	0.28	1.80	1.26
	2	0.08	0.75	1.46		
	3	0.01	0.19	3.38		
3	1	0.06	0.36	1.14	2.50	1.66
	2	0.04	0.64	3.22		
	1	0.05	0.06	0.22	2.49	1.48
	2	0.06	0.46	1.56		
	3	0.03	0.49	3.54		
6	1	0.06	0.33	1.13	2.44	1.57
	2	0.05	0.67	3.09		
	1	0.05	0.05	0.23	2.42	1.38
	2	0.06	0.46	1.62		
	3	0.03	0.48	3.43		

Reduced χ^2 is the "goodness of the fit". "exp num" is the number of exponentials used to fit data; "α" is the pre-exponential factor; "f" is the fraction of the lifetime and "τ" is the fluorescence lifetime. Error for calculated fluorescence lifetimes is between 5–15% for each parameter. Equation 2 was used for fitting data and average fluorescence lifetime was calculated according to Eq. 3

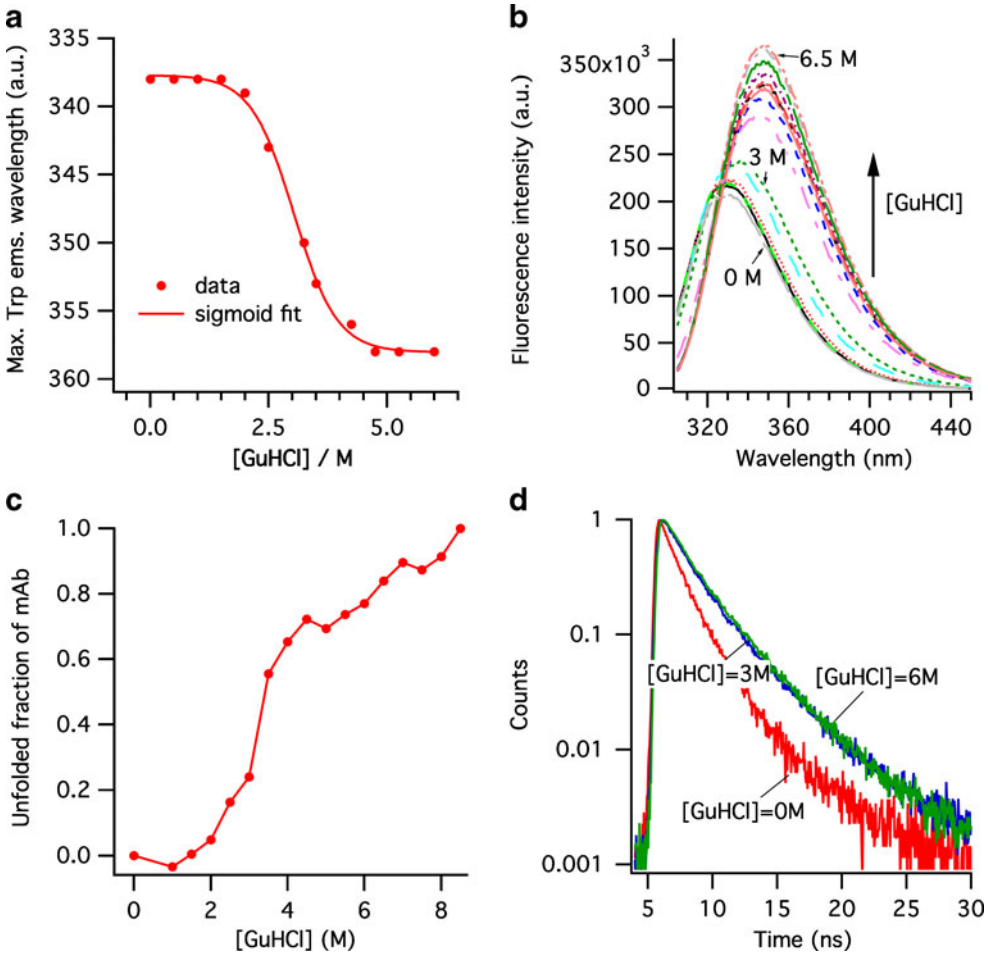

Fig. 3 GuHCl unfolding of mAbs. **a** Sigmoid fit to steady-state emission data. The mid-point of the unfolding curve is at [GuHCl]=3 M; **b** Change of emission spectra with GuHCl concentration; **c** Fraction of unfolded mAb with GuHCl concentration. Lines are to guide to the eye; **d** Fluorescence lifetime as a function of GuHCl concentration. The fluorescence decay curve fit results are shown in Table 1

could become close enough to satisfy energy transfer. Figure 4 (b) shows such dynamical behavior over 30 ns for some of Trp distances smaller than 20 Å. This means that conformational fluctuations may permit dipole-dipole interactions between Trp residues. Besides, we calculated Trp-Trp distances from the middle of bond that connects benzene ring with indole ring in Trp residues. Further evaluation of distances between Trps in the crystal structure revealed that distances between some carbon atoms among some Trp residues are much closer than the distances shown in Fig. 4(b). For example, benzene rings could be within 4–6 Å distance from one another (e.g., between the indole-ring Carbon atoms) but the measured distance between the same Trp residues could be more than 10 Å if it is measured from the Trp middle points (Supplementary Figure 1). It is known that, both of the excited state dipoles of Trp are linearly aligned along the Trp structure (though with about 95° angle) [23, 70]. Hence dipole-dipole interactions could take place if dipoles from two neighboring Trps are close enough at the edges but not from the middle points. Therefore, estimating the presence of energy transfer solely from calculated Trp-Trp distances from the middle of the Trp residues in the crystal structure could be misleading and, thus, each Trp-Trp distance should be inspected in the crystal structure before dismissing the possibility of energy transfer for a particular Trp-Trp pair.

We have also considered intramolecular quenching phenomena, in which closely spaced possible quenchers were determined for each and every Trp residue in the mAb. These quenchers can be side chains as well as surrounding water molecules. Barkley and co-workers determined possible amino acid quenchers of Trp in solution [71, 72]. According to their findings, eight amino acids (i.e., Cys, Asp, Gly, His, Lys, Asn, Gln, Tyr) as well as water molecules are possible quenchers of Trp fluorescence. We have determined these quencher residues and surrounding solvent molecules within 5 Å from each Trp in crystal structure. Furthermore, every residue and water molecule that comes within 5 Å of a Trp residue was categorized after 15 ns and 30 ns of molecular dynamics simulations (Supplementary Table 3). From this data, we have identified most probable quenched Trp residues, whose fluorescence would almost certainly quench highly (Table 3). These Trp residues are very close to the disulphide bonds as well as Asn residues, and thus distances do not change considerably with time. Trp108

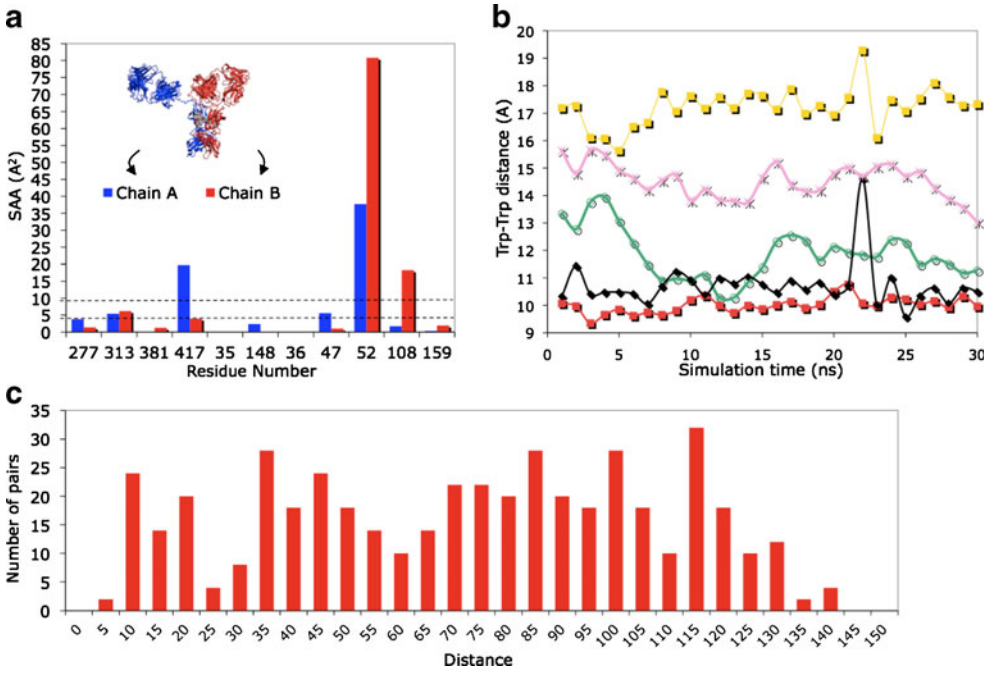

Fig. 4 **a** Solvent accessible area (SAA) of Trp residues in the full mAb. **b** Trp-Trp distance variation with time from molecular dynamics simulation results (only selected are shown). Each colored line represents a unique Trp-Trp pair. Majority of the Trps remain within ±2 Å relative to each other but some show distance change up to ~4–5 Å. **c** The number of Trp-Trp pairs at a given distance. FRET can occur only when donor-acceptor distance is below 15 Å. Therefore, only a few Trp pairs can be involved in FRET

does not seem to be near one of the quencher residues in the crystal structure, but it gets closer to an Asn residue during MD simulations. Hence, Trp108 could also be quenching (Table 3). Likewise, Trp277 transiently comes within 5 Å of Cys321. Whereas Trp277 is within 5 Å of Cys321 in the crystal structure, they move further apart after 15 ns, but return closer than 5 Å after 30 ns of simulation. There are also many water molecules around these Trps as tabulated in Supplementary Table 3. Consequently, their fluorescence would be likely to quench at least partially. We have further identified prospective non-fluorescent Trp residues and listed them in Table 3. It was assumed that if there were Asn or Cys residue within 5 Å distance of a Trp residue, its fluorescence would be highly quenched [73]. Based on these results, we can say that not all Trp residues would contribute equally to the overall protein fluorescence.

Simulation of Energy Transfer with a Master Equation We simulated fluorescence anisotropy in order to determine whether or not energy transfer among Trps could cause the observed loss of fluorescence depolarization. The residue index number of some Trp pairs that could be involved in

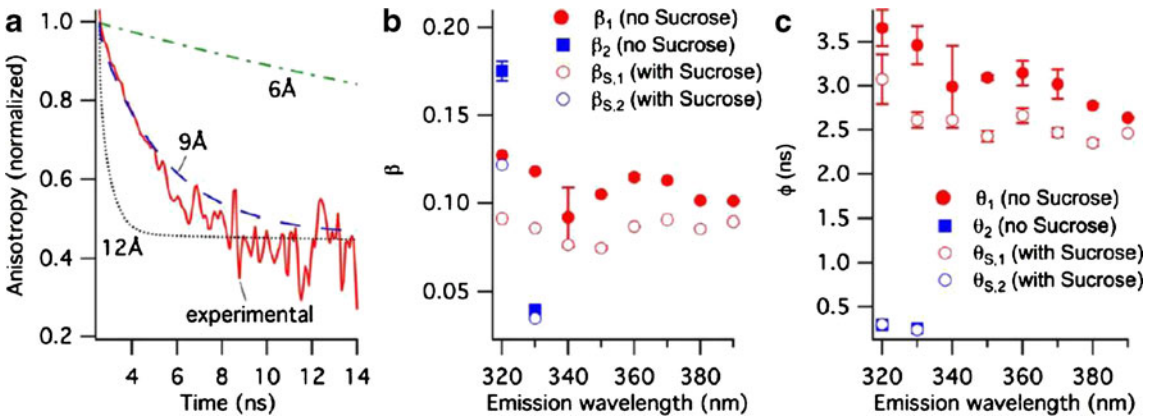

Fig. 5 **a** Comparison of experimental and simulated anisotropy. The data are normalized to unity at zero time. Anisotropy simulated at different Förster distances are also shown; the best correlation between the experimental and simulated anisotropy is achieved with 9 Å Förster distance. **b** Emission wavelength dependence of pre-exponential factors (*time-zero anisotropies*) for Trp fluorescence anisotropy. **c** Emission wavelength dependence of the experimental Trp fluorescence anisotropy. A single exponential function was used for data analysis with exception to 320 nm and 330 nm data, for which a double exponential fit was necessary. Solutions containing sucrose had 10 times more viscosity (~10 cP) than solutions that did not contain sucrose (~1 cP)

Table 2 Observed and calculated properties of the three classes of Trps with their presumed emission wavelength maxima, observed emission decays and SAA values

Trp position	τ^a (ns)	λ (nm)	SAA (Å^2)
Surface	3.6	≥340	≥10
Partially exposed	1.45	320–340	5–10
Buried	0.27	≤320	≤5

[a] Error for calculated fluorescence lifetimes is between 5–15% for each parameter. Equation 2 was used for fitting data and average fluorescence lifetime was calculated according to Eq. 3

FRET with distances below 15 Å are shown in Fig. 4(c). The simulated anisotropy agrees well with experimental anisotropy indicating that Trp-Trp energy transfer takes place (Fig. 5(a)). The orientational factor κ^2 was calculated for each molecular pair from Trp orientations in the crystal structure. High variation in κ^2 values (not shown) indicates that assuming $\kappa^2 = 2/3$ may also be misleading for multi-Trp proteins although generally this is accepted to be a good approximation for molecules in solution. The fluorescence anisotropy and its pre-exponential factor depend on the emission wavelength are shown in Fig. 5(b, c). In addition to energy transfer between Trps, rotation of Trp residues could also result in loss of depolarization. Therefore, to test whether rotational freedom was the main cause of depolarization, solution viscosity was increased ten times with sucrose (~10 cP). Anisotropy data that were collected below 340 nm could be analyzed with a double exponential function with one fast and one slow rotational correlation times. Anisotropy that is collected above 340 nm is described only by a single exponential function (Fig. 5(c) and Supplementary Table 2) both in the presence and absence of sucrose. Increasing the viscosity limits rotational freedom of the Trp residues. Therefore, anisotropy is not expected to decrease in the presence of sucrose. However, increasing the viscosity should have no effect on anisotropy if the depolarization is due to energy transfer rather than rotational movement. Figure 5(c) shows that fast decay is insensitive to the viscosity increase below 340 nm. This indicates that fast rotational correlation time is not due to rotational movement of Trp residues. Even the longer correlation time is affected less compared to 340 nm observations. This shows that depolarization at these lower wavelength should be due to energy transfer. In contrast, anisotropy values depend heavily on viscosity above 340 nm (Fig. 5(c)). This is expected since depolarization of the solvent exposed Trp residues are mainly due to local rotation of Trps in a 'wobbling in a cone' motion.

We have also calculated energy transfer percentages and directions to identify possible Tr-Trp energy transfer pairs from master equation simulations (Supplementary Table 4). Since Trp residues that are in close proximity by 5 Å or less to Cys or Asn residues are hypothesized not to be fluorescent, these Trps would not be able to participate in energy transfer as donors due to being highly quenched by these residues. But these Trps would still be able to act like an acceptor, more specifically as traps and there would be no back transfer from these Trps. Based on these assumptions, energy transfer between Trp313-Trp277, Trp417-Trp381, Trp313-Trp277, Trp108-Trp35/36/52, and Trp47-Trp35/36 would take place in the forward direction (the first Trp is donor and the second one is acceptor).

There are only two pairs which are not affected by the nearby Cys or Asn residues: one pair is Trp417A-Trp417B with only 2% calculated transfer efficiency, and the other pair is Trp108-Trp47 with 28% transfer efficiency. Note that energy transfer may occur in both directions for these two pairs.

Conclusion

Understanding Trp fluorescence in therapeutic mAbs is crucial because intrinsic protein fluorescence spectroscopy is one of the most commonly used methods for studying protein stability and dynamics. Multi-Trp proteins suffer from the complexity of measured emission because each Trp contributes to the fluorescence somewhat differently. In addition, the heavy dependence of Trp fluorescence on its surrounding polarity further contributes to this complexity. We examined Trp fluorescence in detail via fluorescence

Table 3 Non-fluorescent Trp residues according to data from supplementary table. Only amino acid residues were taken as quenchers and non-fluorescent Trps were identified if these quenchers existed within ≤5 Å sphere around Trp in the X-Ray structure or existed in 30 ns MD simulations

X-Ray structure			MD simulations		
Trp	Quencher	Distance (Å) Chain A/Chain B	Trp	Quencher	Distance (Å) Chain A/Chain B
35	Cys	3.9/4.5	35	Cys	4.2/4.6
52	Asn	4.7/4.7	36	Cys	3.8/4.9
148	Cys	3.8/3.6	148	Cys	4.4/4.8
159	Cys	3.9/4.0	159	Cys	4.7/4.5
277	Cys	4.4/5.0	277	Cys	4.7/4.3
381	Cys	5.0/3.8	381	Cys&Asn	4.6/4.5

lifetime, anisotropy, quenching, and master equation simulation, and observed that energy transfer occurs between Trp residues.

Furthermore, we propose that Trps can be categorized according to their rigidity and water accessibility within the mAb structure [43, 64–66, 74–79]. The evidence presented here suggests that three types of Trps exist in the protein matrix—Trp properties are shown in Table 2. Surface Trp residues have very high flexibility as well as high solvent accessibility. A number of Trp residues are buried in the core of the protein and, thus, do not have much flexibility or solvent accessibility. These two types of emitters have different fluorescence emission: emission of buried Trps is blue-shifted while surface Trps fluoresce at the red side of the spectrum, around 350 nm. A water solvable quencher such as acrylamide easily quenches the surface Trps but cannot access the buried Trp residues. Another class of Trp residues lies between these two extremes, exhibiting partial exposure to solvent. This type can be quenched up to a certain level by increasing quencher concentration.

Energy transfer between different Trp classes as well as among Trps within a particular class is a possibility in therapeutic mAbs. Energy transfer between Trps is a reasonable explanation for the interior Trps having very short lifetimes. Energy transfer could be one of the main quenching mechanisms for the emission of buried Trps provided that there is no other excited state reaction taking place.

Acknowledgment We thank Prof. GS Beddard (Univ. of Leeds, UK) for his help with the energy migration routine, valuable discussions and critical reading the manuscript. Dr. M Dogan (SRL, Inc., MA) is acknowledged for valuable discussions, and Bob Chen (ChE, MIT) is acknowledged for technical help. We thank Novartis for financial support.

References

1. Visser NV, Westphal AH, van Hoek A, van Mierlo CPM, Visser AJWG, van Amerongen H (2008) Tryptophan-tryptophan energy migration as a tool to follow apoflavodoxin folding. Biophys J 95:2462–2469
2. Togashi D, Ryder A (2008) A fluorescence analysis of ANS bound to bovine serum albumin: binding properties revisited by using energy transfer. J Fluoresc 18:519–526
3. Efendiev R, Cinelli AR, Leibiger IB, Bertorello AM, Pedemonte CH (2006) FRET analysis reveals a critical conformational change within the Na, K-ATPase [alpha]1 subunit N-terminus during GPCR-dependent endocytosis. FEBS Lett 580:5067–5070
4. Moens PDJ, Helms MK, Jameson DM (2004) Detection of tryptophan to tryptophan energy transfer in proteins. Protein J 23:79–83
5. Kayser V, Turton DA, Aggeli A, Beevers A, Reid GD, Beddard GS (2004) Energy migration in novel pH-Triggered self-assembled beta-sheet ribbons. J Am Chem Soc 126:336–343
6. Beyer CF, Gibbons WA, Craig LC, Longworth JW (1974) Heterogeneous tryptophan environments in the cyclic peptides tyrocidines B and C. Phosphorescence studies. J Biol Chem 249:3204–3211
7. Desie G, Boens N (1986) Study of the time-resolved tryptophan fluorescence of crystalline.alpha.-chymotrypsin. Biochemistry 25:8301–8308
8. Gakamsky DM, Haas E, Robbins P, Strominger JL, Pecht I (1995) Selective steady-state and time-resolved fluorescence spectroscopy of an HLA-A2-peptide complex. Immunol Lett 44:195–201
9. Imoto T, Forster LS, Rupley JA, Tanaka F (1972) Fluorescence of lysozyme. Emissions from tryptophan residues 62 and 108 and energy migration. Proc Nat Acad Sci USA 69:1151–1155
10. Pandit A, Fay N, Bordes L, ValÈry C, Cherif-Cheikh R, Robert B, Artzner F, Paternostre M (2008) Self-assembly of the octapeptide lanreotide and lanreotide-based derivatives: the role of the aromatic residues. J Pept Sci 14:66–75
11. Toulme JJ, Le Doan T, Helene C (1984) Role of tryptophyl residues in the binding of gene 32 protein from phage T4 to single-stranded DNA. Photochemical modification of tryptophan by trichloroethanol. Biochemistry 23:1195–1201
12. Watanabe F, Jameson DM, Uyeda K (1996) Enzymatic and fluorescence studies of four single-tryptophan mutants of rat testis fructose 6-phosphate, 2-kinase:fructose 2, 6-bisphosphatase. Protein Sci 5:904–913
13. Weber G (1960) Fluorescence-polarization spectrum and electronic-energy transfer in proteins. Biochem J 75:345–352
14. Weber G (1960) Fluorescence-polarization spectrum and electronic-energy transfer in tyrosine, tryptophan and related compounds. Biochem J 75:335–345
15. Lakowicz JR (2006) Principles of fluorescence spectroscopy. Springer, New York
16. Willaert K, Loewenthal R, Sancho J, Froeyen M, Fersht A, Engelborghs Y (1992) Determination of the excited-state lifetimes of the tryptophan residues in barnase, via multifrequency phase fluorometry of tryptophan mutants. Biochemistry 31:711–716
17. Lakowicz JR, Cherek H, Gryczynski I, Joshi N, Johnson ML (1987) Enhanced resolution of fluorescence anisotropy decays by simultaneous analysis of progressively quenched samples. Applications to anisotropic rotations and to protein dynamics. Biophys J 51:755–768
18. Karreman G, Steele RH, Szent-Gyorgyi A (1958) On resonance transfer of excitation energy between aromatic aminoacids in proteins. Proc Natl Acad Sci USA 44:140
19. Eisinger J, Feuer B, Lamola AA (1969) Intramolecular singlet excitation transfer. Applications to polypeptides. Biochemistry 8:3908–3915
20. Tran CD, Beddard GS (1985) Studies of the fluorescence from tryptophan in melittin. Eur Biophys J Biophys Lett 13:59–64
21. Petrich JW, Longworth JW, Fleming GR (1987) Internal motion and electron transfer in proteins: a picosecond fluorescence study of three homologous azurins. Biochemistry 26:2711–2722
22. Fleming GR, Morris JM, Robbins RJ, Woolfe GJ, Thistlethwaite PJ, Robinson GW (1978) Nonexponential fluorescence decay of aqueous tryptophan and two related peptides by picosecond spectroscopy. Proc Natl Acad Sci USA 75:4652–6
23. Vivian JT, Callis PR (2001) Mechanisms of tryptophan fluorescence shifts in proteins. Biophys J 80:2093–2109
24. Beuckeleer KD, Volckaert G, Engelborghs Y (1999) Time resolved fluorescence and phosphorescence properties of the individual tryptophan residues of barnase: evidence for protein-protein interactions. Proteins Struct Funct Genet 36:42–53
25. Engelborghs Y (2004) Time resolved protein fluorescence. Application to multi-tryptophan proteins. Supramol. Struct. Funct. 8, [Proc. Int. Summer Sch. Biophys.], 8th, 73–98

26. Carter PJ (2006) Potent antibody therapeutics by design. Nat Rev Immunol 6:343–357
27. Walsh G (2007) Pharmaceutical biotechnology: concepts and applications. Wiley, Chichester
28. Groves MJ (2006) Some challeges relating to the future of biopharmaceutical technology. In: Groves MJ (ed) Pharmaceutical biotechnology. Taylor & Francis Group, LLC, Boca Raton, pp 389–396
29. Vollrath F (2000) Strength and structure of spiders' silks. Rev Mol Biotechnol 74:67–83
30. Zelent B, Kusba J, Gryczynski I, Johnson ML, Lakowicz JR (1998) Time-resolved and steady-state fluorescence quenching of *N*-acetyl-L-tryptophanamide by acrylamide and iodide. Biophys Chem 73:53–75
31. Eftink MR, Ghiron CA (1976) Exposure of tryptophanyl residues in proteins. Quantitative determination by fluorescence quenching studies. Biochemistry 15:672–680
32. Gryczynski I, Wiczk W, Johnson ML, Lakowicz JR (1988) Lifetime distributions and anisotropy decays of indole fluorescence in cyclohexane/ethanol mixtures by frequency-domain fluorometry. Biophys Chem 32:173–185
33. Szabo AG, Stepanik TM, Wayner DM, Young NM (1983) Conformational heterogeneity of the copper binding site in azurin. A time-resolved fluorescence study. Biophys J 41:233–244
34. Callis PR, Brand L, Johnson ML (1997) 1La and 1Lb transitions of tryptophan: applications of theory and experimental observations to fluorescence of proteins. In Methods in Enzymology ed. ^eds), pp. 113–150. Academic Press
35. Beddard GS, Tran CD (1985) Fluorescence studies of the restricted motion of tryptophan in alpha -cobratoxin. Eur Biophys J 11:243–248
36. Petrich JW, Chang MC, Mcdonald DB, Fleming GR (1983) J Am Chem Soc 105:3824–3832
37. Edelhoch H, Brand L, Wilchek M (1967) Fluorescence studies with tryptophyl peptides. Biochemistry 6:547–59
38. Edelhoch H, Bernstein RS, Wilchek M (1968) The fluorescence of tyrosyl and tryptophanyl diketopiperazines. J Biol Chem 243:5985–92
39. Steinberg IZ (1971) Long-range nonradiative transfer of electronic excitation energy in proteins and polypeptides. Annu Rev Biochem 40:83–114
40. Cowgill RW (1963) Fluorescence and the structure of proteins. II. Fluorescence of peptides containing tryptophan or tyrosine. Biochim Biophys Acta 75:272–273
41. Cowgill RW (1963) Fluorescence and the structure of proteins. I. Effects of substituents on the fluorescence of indole and phenol compounds. Arch Biochem Biophys 100:36–44
42. Burstein EA, Abornev SM, Reshetnyak YK (2001) Decomposition of protein tryptophan fluorescence spectra into log-normal components. I. Decomposition algorithms. Biophys J 81:1699–1709
43. Reshetnyak YK, Andreev OA, Borejdo J, Toptygin DD, Brand L, Burstein EA (2000) The identification of tryptophan residues responsible for ATP-induced increase in intrinsic fluorescence of myosin subfragment 1. J Biomol Struct Dyn 18:113–126
44. Reshetnyak YK, Burstein EA (2001) Decomposition of protein tryptophan fluorescence spectra into log-normal components. II. The statistical proof of discreteness of tryptophan classes in proteins. Biophys J 81:1710–1734
45. Reshetnyak YK, Koshevnik Y, Burstein EA (2001) Decomposition of protein tryptophan fluorescence spectra into log-normal components. III. Correlation between fluorescence and microenvironment parameters of individual tryptophan residues. Biophys J 81:1735–1758
46. Di Muro P, Beltramini M, Nikolov P, Petkova I, Salvato B, Ricchelli F (2002) Fluorescence spectroscopy of the tryptophan microenvironment in Carcinus aestuarii hemocyanin. Z Naturforsch C 57:1084–91
47. Bradforth SE, Jimenez R, van Mourik F, van Grondelle R, Fleming GR (1995) Excitation transfer in the core light-harvesting complex (LH-1) of Rhodobacter sphaeroides: an ultrafast fluorescence depolarization and annihilation study. J Phys Chem 99:16179–16191
48. Jimenez R, Dikshit SN, Bradforth SE, Fleming GR (1996) Electronic excitation transfer in the LH2 complex of rhodobacter sphaeroides. J Phys Chem 100:6825–6834
49. Andrews DL, Demidov AA (1999) Resonance energy transfer. Wiley, Canada
50. Ghiron CA, Longworth JW (1979) Transfer of singlet energy within trypsin. Biochemistry 18:3828–32
51. Saphire EO et al (2001) Crystal structure of a neutralizing human IgG against HIV-1: a template for vaccine design. Science 293:1155–1159
52. O'Connor DV, Phillips D (1984) Time-correlated single-photon counting. Academic, London
53. Lehrer S (1971) Solute perturbation of protein fluorescence. Quenching of the tryptophyl fluorescence of model compounds and of lysozyme by iodide ion. Biochemistry 10:3254–3263
54. Förster T (1948) Zwischenmolekulare energiewanderung und fluoreszenz (trans: Intermolecular energy migration and fluorescence). Ann Phys 2:55–75
55. Förster T (1959) Transfer mechanisms of electronic excitation. Discuss Faraday Soc 27:7–17
56. Förster T (1965) Delocalized excitation and excitation transfer. In: Sinanoglu O (ed) Modern quantum chemistry. Istanbul lectures. Part III: action of light and organic crystals. Academic, New York, pp 93–137
57. Brooks BR, Bruccoleri RE, Olafson BD, States DJ, Swaminathan S, Karplus M (1983) CHARMM: a program for macromolecular energy, minimization, and dynamics calculations. J Comput Chem 4:187–217
58. Phillips JC et al (2005) Scalable molecular dynamics with NAMD. J Comput Chem 26:1781–1802
59. MacKerell AD Jr et al (1998) All-atom empirical potential for molecular modeling and dynamics studies of proteins. J Phys Chem B 102:3586–3616
60. Jorgensen WL, Chandrasekhar J, Madura JD, Impey RW, Klein ML (1983) Comparison of simple potential functions for simulating liquid water. J Chem Phys 79:926–35
61. Kuttel M, Brady JW, Naidoo KJ (2002) Carbohydrate solution simulations: producing a force field with experimentally consistent primary alcohol rotational frequencies and populations. J Comput Chem 23:1236–1243
62. Eftink MR (1992) Fluorescence quenching: theory and applications. In: Lakowicz JR (ed) Topics in fluorescence spectroscopy. Kluwer Academic Publishers, New York, pp 52–126
63. Eftink MR, Ghiron CA (1977) Exposure of tryptophanyl residues and protein dynamics. Biochemistry 16:5546–5551
64. Beechem JM, Brand L (1985) Time-resolved fluorescence of proteins. Annu Rev Biochem 54:43–71
65. Nishimoto E, Yamashita S, Szabo AG, Imoto T (1998) Internal motion of lysozyme studied by time-resolved fluorescence depolarization of tryptophan residues. Biochemistry 37:5599–5607
66. Stryjewski W, Wasylewski Z (1986) The resolution of heterogeneous fluorescence of multitryptophan-containing proteins studied by a fluorescence-quenching method. Eur J Biochem 158:547–553
67. Kumar S, Swaminathan R (2007) Employing the fluorescence anisotropy and quenching kinetics of tryptophan to hunt for residual structures in denatured proteins. J Chem Sci 119:141–145
68. Lakowicz JR, Weber G (1980) Nanosecond segmental mobilities of tryptophan residues in proteins observed by lifetime-resolved fluorescence anisotropies. Biophys J 32:591–601

69. Ionescu RM, Vlasak J, Price C, Kirchmeier M (2008) Contribution of variable domains to the stability of humanized IgG1 monoclonal antibodies. J Pharm Sci 97:1414–1426
70. Callis PR (1991) Molecular orbital theory of the [sup 1]L[sub b] and [sup 1]L[sub a] states of indole. J Chem Phys 95:4230–4240
71. Yu H-T, Vela MA, Fronczek FR, McLaughlin ML, Barkley MD (1995) Microenvironmental effects on the solvent quenching rate in constrained tryptophan derivatives. J Am Chem Soc 117:348–357
72. Chen Y, Barkley MD (1998) Toward understanding tryptophan fluorescence in proteins. Biochemistry 37:9976–9982
73. Bismuto E, Martelli PL, Casadio R, Irace G (2000) Tryptophanyl fluorescence lifetime distribution of hyperthermophilic beta-glycosidase from molecular dynamics simulation: a comparison with the experimental data. Protein Sci 9:1730–42
74. Provencher SW, Dovi VG (1979) Direct analysis of continuous relaxation spectra. J Biochem Biophys Meth 1:313–318
75. Deerfield DW, Holland-Minkley AM, Geigel J, Nicholas HB (1997) Classification of the environment of protein residues. J Protein Chem 16:441–447
76. Foresta B, Champeil P, Maire M (1990) Different classes of tryptophan residues involved in the conformational changes characteristic of the sarcoplasmic reticulum Ca²⁺-ATPase cycle. Eur J Biochem 194:383–388
77. Malvezzi-Campeggi F, Rosato N, Finazzi-AgrÚ A, Maccarrone M (2001) Effect of denaturants on the structural properties of soybean lipoxygenase-1. Biochem Biophys Res Commun 289:1295–1300
78. Patanjali SR, Swamy MJ, Surolia A (1987) Studies on tryptophan residues of Abrus agglutinin. Stopped-flow kinetics of modification and fluorescence-quenching studies. Biochem J 243:79–86
79. Venere AD, Mei G, Gilardi G, Rosato N, Matteis FD, McKay R, Gratton E, Agrò AF (1998) Resolution of the heterogeneous fluorescence in multi-tryptophan proteins: ascorbate oxidase. Eur J Biochem 257:337–343